

K*-shell vacancies and residual excitation in heavy ions penetrating solids

Forrest Hopkins, Jonathan Sokolov, and Andrew Little

Department of Physics, State University of New York, Stony Brook, New York 11794

(Received 3 June 1976)

Measurements of *K* vacancies of F, S, and Cl ions penetrating various solids at MeV/amu energies indicate that the formation of those vacancies is well described by a simple model of competing *K*-shell rearrangement processes. Specifically, the progression at increasing penetration depth toward equilibrium vacancy fractions and the magnitudes of the fractions themselves find quantitative agreement in the model. The observation of substantial residual excitation in Cl and S at 2 MeV/amu implies that *K* relaxation via Auger transitions is a significant post-foil charge-changing mechanism for those ions. Equilibrium effects previously taken to be due to dynamic screening by target electrons are herein attributed to the *K*-equilibrium process.

I. INTRODUCTION

The determination of the states of energetic ions as they traverse solids has long been one of the most interesting and challenging aspects of ion-atom collisions.¹ Much of the experimental information available is concerned with quantities measured after emergence of ions from thin solid foils, such as charge-state distributions. The extrapolation from such post-foil measurements back to the interior of the solid is often uncertain in view of the possibilities of collisional rearrangement at the surface and relaxation of excited states via photon and Auger electron emission at very short distances and times beyond the foils.

One internal phenomenon for which precise measurements do exist is energy loss. A primary finding¹ experimentally is that, for many cases, stopping powers are relatively insensitive to the medium, i.e., gaseous and solid materials yield about the same results. To the extent that energy loss is sensitive to screening effects due to attached electrons, such results imply at most small differences in the effective charge of the ion in the various environments. An apparently contradictory finding is that equilibrium charge-state distributions of ions emerging from solids for many of the cases above are centered appreciably higher than those emerging from gases.

Attempts to explain the latter effect have taken primarily two directions, the domains of which and validity of which have yet to be confirmed. Both find justification in the extremely short collision times experienced by the ion in the dense solid medium, times which may approach and be shorter than characteristic transition lifetimes and so represent an added dimension to the dynamics in the gaseous medium. The Bohr-Lindhard (BL) theory² attributes the higher degree of ionization to the pumping up through consecutive collisions of inner-shell electrons to the loosely

bound outer shells where they are more easily ionized. The distribution emerging from the solid is very nearly that established in the solid; hence it is essentially a "ground-state" distribution. The Betz-Grodzins (BG) model³ envisions a preponderance of excited states at equilibrium in the interior, a large fraction of which Auger-decay beyond the solid, thereby increasing charge states. Thus while the charge is lower inside the solid, the additional electrons would not necessarily alter the stopping power in a major way. It should be kept in mind that both processes can contribute to observed charge-state effects in a given situation.

Several experiments⁴⁻⁹ within the past few years have utilized either projectile or target x-ray emission from within a solid to deduce something about the states of the projectile. The present paper is an extension of one of those efforts⁷ to include a more comprehensive set of data concerning the presence of *K* vacancies in various ions penetrating solids. In particular, the *K* vacancy fractions for F, S, and Cl beams at ~MeV/amu energies in C and also Cl in various other materials have been measured and have been found to be adequately described by equilibrium effects expected based on cross sections for creating and filling vacancies in the *K* shell for the projectile, i.e., competing *K*-shell rearrangement cross sections. The latter cross sections have been extrapolated from previously available experimental information for very similar systems. Substantial residual *K*-shell excitation is indicated for the S and Cl ions, the loss of which presumably constitutes a significant increase in charge state for the emerging beams in the manner proposed by Betz and Grodzins.³ For the case of Cl in C, we find that the production of metastable Cl *K* transitions, observed beyond thin C foils of various thicknesses, tracks the equilibrium curve describing the vacancy fraction as a function of penetration depth. We also pro-

pose that the FK equilibrium process accounts for thickness-dependent effects in target x-ray production for a similar system previously attributed to dynamic screening by target valence electrons.

II. EXPERIMENTAL METHOD

The measurements here have been accomplished by using ultra-thin solid probe layers of elements whose K x-ray cross sections are sensitive primarily to vacancies in the K shell of the projectile, i.e., are relatively insensitive to the presence of attached electrons in the L and outer shells. The probe layers were evaporated directly onto solid foils of interest, e.g., a C foil, and were kept thin enough to insure a minimum of K -shell rearrangement in the beam during its traversal of the layer. Thus the x-ray yield induced in the layer reflected in a direct way the state of the beam, insofar as K vacancies were concerned, after penetration of a given thickness of medium or following emergence from a prefoil. The probe layers fulfilling these requirements were $\sim 1 \mu\text{g}/\text{cm}^2$ of Cu for Cl and S and $\sim 1 \mu\text{g}/\text{cm}^2$ of Al for F.

The various targets were housed in a stainless-steel target cell which was preceded 15 cm upstream by a 0.32-cm aperture for beam definition. Following the first aperture by 5 cm was an aperture of 0.48-cm diameter which was biased to -300 V to suppress electrons. The target cell and following beamline constituted the beamdump, from which charge integration served as beam monitor. Charge integration was checked by recording elastic scattering from a $\sim 400 \mu\text{g}/\text{cm}^2$ Au foil placed at the target position into a silicon surface-barrier particle detector situated at 90° with respect to the beam. Beamline pressures were typically $\sim 2 \times 10^{-6}$ Torr.

The Al and Cu K x rays were observed with an 80-mm² Si (Li) detector equipped with a 0.00254-cm Be window and possessing ~ 220 -eV resolution for the Mn $K\alpha$ line. For the Al case, the detector was vacuum coupled into the cell at 90° to and 25 cm from the beam axis and was collimated to 0.32 cm. For the Cu runs, the detector was positioned outside the vacuum at 6.5 cm from the target position. A 0.00127-cm-thick Mylar window, a 1-cm air gap, and a 0.0038-cm Al absorber to reduce the predominantly produced beam x rays were placed between target and detector. Processing of signals was done with conventional analog-to-digital conversion and storage on magnetic tape via a PDP-9 computer. Count rates were kept to a few hundred per second, resulting in dead times of at most a few percent, monitored by passing the signal through a single-channel

analyzer prior to conversion.

The F, S, and Cl beams at various incident energies were obtained from the Stony Brook FN tandem Van de Graaff accelerator. To determine the projectile charge-state dependences of the Al K and Cu K cross sections, the beams were post-acceleration stripped by a carbon foil with individual charge states selected out by a 45° switching magnet. A matter of much concern in these experiments was insuring the integrity of the various foils, particularly the probe layers, in view of the well-known debilitating effects of heavy-ion bombardment. Consequently short runs of a few minutes duration were made with low-current beams and repeated several times. Typical currents of ~ 3 nA for S and Cl beams and ~ 10 nA for F provided statistical accuracy within about 3% and resulted in excellent reproducibility.

The several configurations in which measurements were made are shown in Fig. 1. First, the charge-state dependences of x-ray cross sections were recorded. Pure charge states impinged directly onto the probe layer, resulting in target x-ray yields denoted σ_X^Q . The lack of sufficient amounts of Cl^{16+} and S^{15+} from the secondary stripper at the energies reported here necessitated extrapolations based on previous measurements at higher energies, which will be outlined in the following section. The F presented no such problem. Subsequent runs were made where the beam penetrated the backing made of the appropriate material before encountering the probe layer, i.e., the layer faced downstream, as shown in Fig. 1. Relative cross sections measured in this way are hereafter referred to as σ_X^S . Finally measurements were made with the probe layers facing upstream and a prefoil of known thickness placed before the beam collimators a distance of 24 cm from the target position. This configuration, which allowed determination of K vacancies in the ions following

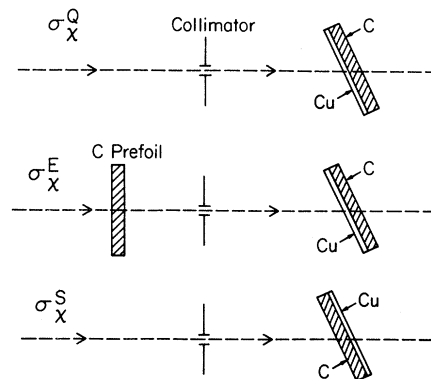


FIG. 1. Experimental configuration for various cross sections.

their emergence from the foils, is denoted σ_x^E . In all cases C prefoils were used.

For the study of S and Cl in C, targets consisted of C foils of thicknesses from $\sim 20 \mu\text{g}/\text{cm}^2$ to $\sim 200 \mu\text{g}/\text{cm}^2$ with a $\sim 1\text{-}\mu\text{g}/\text{cm}^2$ Cu layer evaporated directly onto one side. As will be seen shortly, the above range of thicknesses was needed to reach final values of the equilibrium effects observed. For Cl in the various solids other than C, the targets consisted of $\sim 20\text{-}\mu\text{g}/\text{cm}^2$ C backings, with an intermediate layer of the given material sandwiched between the C and the Cu probe layer. The solids included Al, KCl, Ni, Ge, Ag, and Au, the thicknesses of which varied as discussed in the following section. The data for F in C resulted from Al evaporated on $\sim 20\text{-}\mu\text{g}/\text{cm}^2$ C foils, which were found to be equilibrium thicknesses by checking with results obtained with $50\text{-}\mu\text{g}/\text{cm}^2$ C backings. All of the foil thicknesses were measured via 2.0-MeV proton elastic scattering into the particle detector at 90° . A question which has not been addressed here is the uniformity of the probe layers. We find our results to be consistent with an assumption of uniform thickness.

All the results presented here were obtained with the targets at 30° to the beam axis in the reflection mode indicated in Fig. 1. Essentially the same values were obtained in the transmission mode or with the target angle at 45° . A run in any of the three above configurations was usually followed immediately by a run with the target rotated by 180° . This procedure constituted a self-normalization for each run and provided a consistent way in which to integrate results from several runs over several months time, eliminating systematic errors. The relevant x rays were the Cu $K\alpha$ line and the unresolved Al $K\alpha$ - $K\beta$ lines. The x-ray yields were extracted from photopeak integration reduced by a background determined from a linear least-squares fit to regions on either side of a

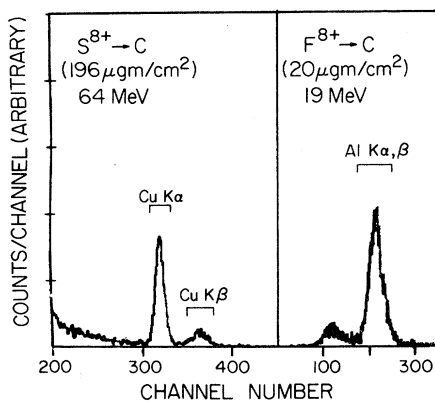


FIG. 2. Spectra of Cu K and Al K x rays.

peak. In one case, for the Ni data, a Gaussian fit to the Cu $K\alpha$ was necessary since it was a small peak on the shoulder of a much larger Ni $K\beta$ line. Spectra for two cases are shown in Fig. 2. The background was more substantial when the higher- Z elements were used.

One measurement reported here of something other than x rays from probe layers involved the observation of metastable Cl K x rays. In that instance the viewing region of the detector was limited to the path of the beam 1 to 3 cm beyond various pure C foils. The Cl K yields, analyzed as described above, were recorded as a function of C foil thickness.

III. MODEL ANALYSIS

In order to be able to discuss in a complete and coherent way the experimental results in the following section, we first present the theoretical framework used here for describing the excitation of an ion penetrating a solid. The formation of vacancies in a particular shell, limited in this paper to the K shell, is governed by the simple rate equation⁶

$$\frac{dY}{dt} = (1 - Y)\sigma_v - Y(\sigma_c + \sigma_r), \quad (1)$$

where Y is the fraction of the beam with K vacancies and is a function of the distance t traversed in the solid, σ_v is the cross section for producing K vacancies, σ_c is the cross section for collisional elimination of the vacancy by processes such as electron capture, and σ_r is an effective filling cross section due to K transitions. The latter is given by $\sigma_r = (n\nu\tau)^{-1}$ where n is the particle density of the medium, ν is the ion velocity, and τ is an average K lifetime where all of the possible excited states with K vacancies are treated as one. The integral of Eq. (1) gives

$$Y(t) = \frac{\sigma_v}{\sigma} [1 - \exp(-\sigma t)], \quad (2)$$

where $\sigma = \sigma_v + \sigma_c + \sigma_r$ and it is assumed that $Y(0) = 0$. At some distance $t \gg \sigma^{-1}$, an equilibrium value of $Y^{\text{eq}} = \sigma_v/\sigma$ is reached.

IV. EXPERIMENTAL DATA AND ANALYSIS

A. Charge-state dependences

The charge-state dependence of the Cu $K\alpha$ x-ray cross section, as reported previously⁷ for the $\sim 1\text{-}\mu\text{g}/\text{cm}^2$ Cu targets, is shown in Fig. 3 for 140-MeV Cl. The cross section shows practically no dependence upon the presence of attached L electrons but takes a substantial jump when the Cl K shell has a vacancy. At the maximum incident

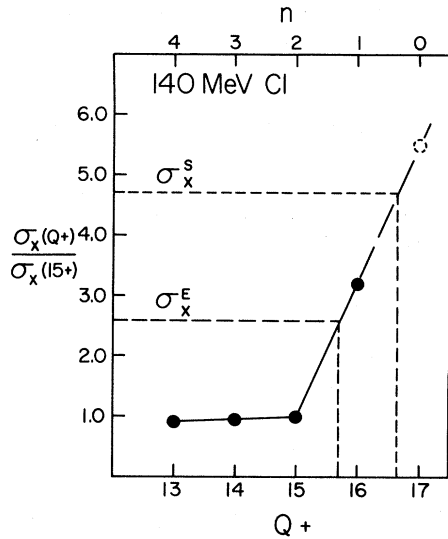


FIG. 3. Dependence of Cu $K\alpha$ x-ray cross section on Cl-charge state at 140 MeV.

energy of 2 MeV/amu discussed in this paper, insufficient amounts of Cl^{16+} and S^{15+} preclude a direct measurement of the variation with K vacancies. However, a previous higher-energy measurement¹⁰ of the Kr K cross section involving few-electron Cl ions incident on Kr under single-collision conditions allows an extrapolation of the 140-MeV results down to 70 MeV. The Kr K -shell binding energy is similar to that of Cu and the dynamics, i.e., importance of K vacancies in the respective vacancy cross sections, over equivalent values of $\eta^{1/2}$ (=projectile velocity/electron velocity), should be similar.

Using such an approach, the σ_x^{16+} magnitude is taken to be $3.2\sigma_x^{15+}$ for Cl. A further extrapolation to obtain the S one-electron value involves the normalization to the data of the Brinkman-Kramers (BK) theoretical expression for electron capture¹¹ from the Cu K shell by the one-electron Cl. That scaling factor is then applied to the prediction for pickup from the Cu K shell by S^{15+} . The latter procedure is a reasonable one in view of the fact that the Kr experiment indicated that the sensitivity to the Cl K vacancy is due to charge exchange from the Kr K shell, alternately the Cu K shell, to the projectile K shell. The resulting σ_x^{15+} for S is $2.2\sigma^{14+}$. Measurements of the Cu K cross section at 2 MeV/amu demonstrated the same lack of dependence of Cl L and $S L$ occupancy as shown in Fig. 3, including Cl^{15+} and S^{14+} .

A measurement of the Al K x-ray cross section as a function of F charge state, using $\sim 1\text{-}\mu\text{g}/\text{cm}^2$ Al targets, is presented in Fig. 4. At energies of 19 MeV, 38 MeV, and 57 MeV, the cross section satisfies the requirement needed for a probe of F

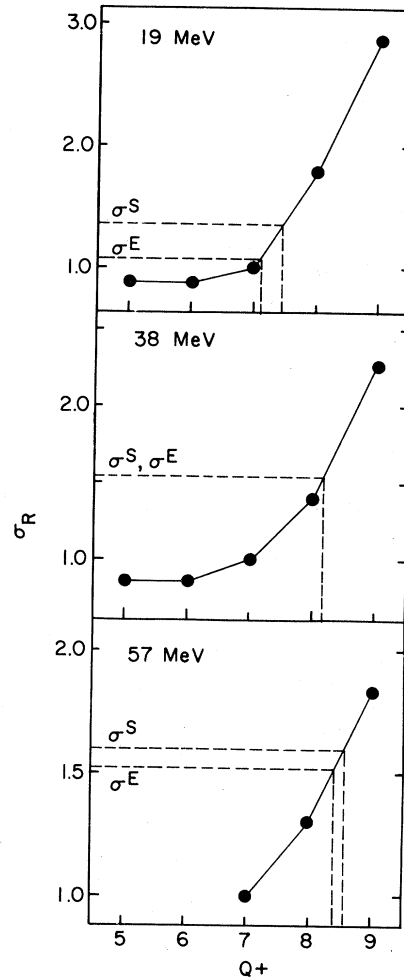


FIG. 4. F charge-state dependence of Al K x-ray cross sections.

K vacancies, i.e., a healthy increase in the yield for F^{8+} and F^{9+} . The observed charge-state dependence is similar to data prepared previously⁴ for O projectiles on several different ultra-thin ($\approx 2\text{-}\mu\text{g}/\text{cm}^2$) Al foils, for which cross sections were essentially the same. That the $1\text{ }\mu\text{g}/\text{cm}^2$ is sufficiently thin to avoid substantial rearrangement of the F K shell is farther indicated by the fact that the observed charge-state dependences are within $\sim 20\%$ of those for the Kr L shell,¹² with a nearly identical binding energy, recorded under single-collision conditions.

B. Vacancy fractions

1. Sulfur and chlorine

Using the indicated increases in probe yields associated with vacancies in the K shell of a given ion, the average number of K vacancies can be deduced in the form of a fraction of the beam ex-

hibiting such excitation. For S the fraction is given by

$$Y(t) = (\sigma_{\chi}^S - \sigma_{\chi}^{14+}) / \sigma_{\chi}^K, \quad (3)$$

where t is the depth of penetration in the σ_{χ}^S mode and $\sigma_{\chi}^K = 2(\sigma_{\chi}^{15+} - \sigma_{\chi}^{14+})$ is the yield arising from a fully vacant S K shell. The data as taken for the case of 64-MeV S in C is shown in Fig. 5(a), where the ratio of σ_{χ}^S to σ_{χ}^K was recorded. The σ_{χ}^S yields increase as the thickness of the C is increased, eventually reaching a saturation value. The equivalent K -vacancy fractions are displayed in Fig. 5(b), with an equilibrium value $Y^{eq} \approx 0.5$ reached by a C thickness of $\sim 200 \mu\text{g}/\text{cm}^2$. Thus on the average each S ion has about one K vacancy at equilibrium in the solid ($Y^{eq} = 1.0$ would indicate a fully vacant K shell). The behavior is similar to that for 70-MeV Cl reported earlier,⁷ where $Y^{eq} = 0.35$. The error bar in Fig. 5 is indicative of the typical repeatability for the data, which is thought to be limited by target considerations such as the uniformity of the probe layer.

The theoretical curve for the K equilibrium process generated from Eq. (2) is included in Fig. 5(b). The cross sections used were 4.4×10^{-19} , 4.4×10^{-19} , and $0.17 \times 10^{-19} \text{ cm}^2$ for σ_v , σ_r , and σ_c , respectively. The value for σ_v in C has been estimated from O-induced S K -shell vacancy production¹³ by a $(\frac{6}{8})^2$ scaling of the velocity-matched values of those cross sections. The Z^2 scaling procedure, which is used throughout this paper when extrapolating to obtain vacancy cross sections, is based on an assumption⁴ of quadratic dependence on the nuclear charge of the ionizing atom and should be reasonably valid for asymmetric collisions. The average lifetime τ measured by Betz *et al.*⁸ for S of 1.4×10^{-14} sec has been used for σ_r . The electron-capture magnitude

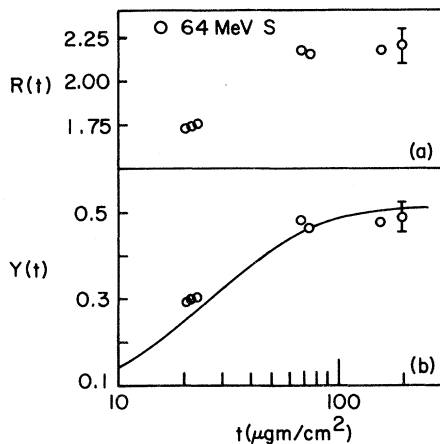


FIG. 5. Experimental and theoretical descriptions of S K -vacancy fraction.

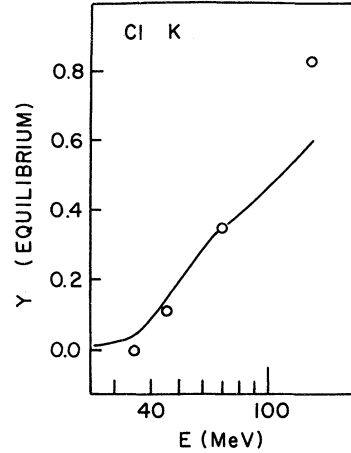


FIG. 6. Energy dependence of Y^{eq} for Cl in C.

is based on a scaling by 0.1 for the BK expression from Nikolaev¹¹ for K pickup, a scaling factor which is in line with earlier work.^{10,12} It is important to note that the capture is nearly negligible for this situation, i.e., the nature of the curve in Fig. 5(b) is determined primarily by σ_v and σ_r . The agreement with experiment is excellent, perhaps somewhat fortuitously in view of the many assumptions in both the data analysis and the determination of the rearrangement cross sections. However the trends of the vacancy fraction are clearly predicted by the simple model.

The values Y^{eq} for Cl in C as a function of energy are presented in Fig. 6. The point at 140 MeV is from a previous experiment.⁷ At the lower energies a maximum C thickness of $50 \mu\text{g}/\text{cm}^2$ was used, as the energy loss of the beam at those velocities introduces some uncertainty in the Cu K cross sections. Additional uncertainty arises from the fact that the same relative yield of $\sigma_{\chi}^{16+} = 3.2 \sigma^{15+}$ was assumed in a region where the extrapolation could be in serious error. However, it is evident that the K excitation is drastically reduced with decreasing energy.

The appropriate theoretical curve for $Y^{eq} = \sigma_v / \sigma$ using the magnitudes in Table I exhibits the same behavior as the data. The Cl vacancy cross sections have been derived as described above by the $(\frac{6}{8})^2$ scaling of the S cross sections¹³ in addition to appropriate corrections for the different values of the K binding energy and $\eta^{1/2}$, according to the binary encounter approximation (BEA).¹⁴ The lifetime τ was obtained by scaling the S value by the ratio of the theoretical single vacancy K rates for Cl and S from McGuire.¹⁵ As with S, σ_c is equal to the BK value scaled by 0.1 and again is of minor importance. It should be pointed out that τ is expected to be a function of the incident energy, as it depends on the configurations of the

TABLE I. K rearrangement cross sections for Cl in C.

E (MeV)	σ_v (10^{-19} cm 2)	σ_r (10^{-19} cm 2)
35	0.247	6.52
40	0.605	6.10
45	0.937	5.75
55	1.57	5.20
60	1.92	4.98
70	2.44	4.61
90	2.99	4.07
110	3.54	3.68
125	4.32	3.45
140	5.03	3.26

various K -shell excited states of the projectile produced in the solid and is sensitive therefore to the L -shell and outer-shell occupation. At higher energies where few electron states and thereby longer individual lifetimes become important the value of τ presumably increases substantially. The fact that we have used here a single value for all energies may account for the underestimate of the vacancy fraction at 140 MeV, as seen in Fig. 6.

Measurements of Y^{eq} for Cl at 70 MeV in a variety of solids is shown in Fig. 7(b). The targets in

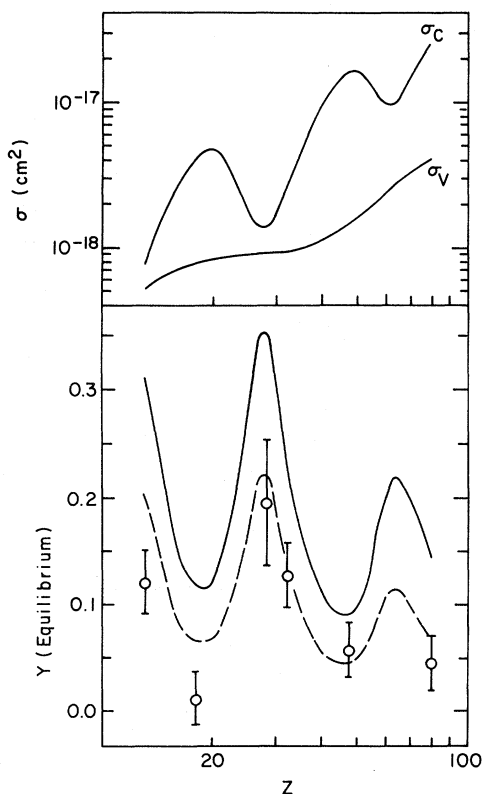


FIG. 7. Z dependence of Y^{eq} for Cl in a variety of solids at 70 MeV.

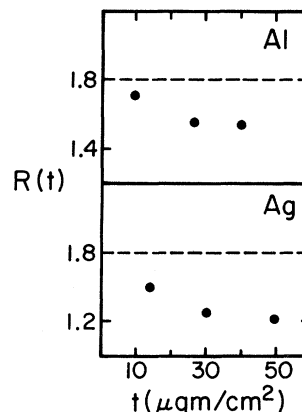


FIG. 8. Thickness dependence of $Y(t)$ for 70-MeV Cl in Al and Ag.

these cases consisted of a particular medium sandwiched between a $20\text{-}\mu\text{g}/\text{cm}^2$ C backing and a Cu probe layer. Thus in the σ_x^s mode, the beam reached some value of $Y(t)$ in the first C layer and then readjusted in the intermediate layer before striking the Cu. The data as taken for various thicknesses of Al and Ag are shown in Fig. 8. Since the equilibrium values of $Y(t)$ are in fact lower than those expected after $20\text{ }\mu\text{g}/\text{cm}^2$ of C, the data start above and drop down to Y^{eq} with increasing thickness. Single thicknesses of $41.8\text{-}\mu\text{g}/\text{cm}^2$ of KCl, $29.0\text{ }\mu\text{g}/\text{cm}^2$ of Ge, and $27.3\text{ }\mu\text{g}/\text{cm}^2$ for Au were used, which according to the magnitudes of the cross sections to be discussed in the next paragraph should yield values of $Y(t)$ which are essentially equilibrium. A somewhat less than equilibrium Ni thickness of $12.7\text{ }\mu\text{g}/\text{cm}^2$ was necessitated by the fact that the Cu $K\alpha$ line coincided with the Ni $K\beta$, introducing the large error depicted in Fig. 7(b), which arose from the fit to obtain the x-ray yield. However essentially no change of $Y(t)$ in the Ni from that expected after penetration through the C backing was observed and so the point is included as a tentative value.

It is apparent that the K excitation in all of these solids is below the fraction of 0.35 measured for C. The rearrangement cross sections σ_v and σ_c are shown graphically in Fig. 7(a). The σ_c curve is the BK curve for capture to the Cl K shell as a function of the Z of the solid, scaled by 0.07, a normalization which was found to be appropriate to describe the electron-capture magnitudes observed for the Cl-Kr collisions.¹⁰ More careful attention must be given to the charge-exchange component as it is the dominant K filling process for $Z \geq 13$. The values of σ_r are not shown here, as in every case they are a small fraction of σ_c . However, they are included in the equilibrium curve in Fig. 7(b). It should be remembered that the curve in Fig. 7(b) is applicable only to solids

and is drawn through points for Z values of gaseous elements simply to connect the points for the solid values. The values of σ_v are based on Cl K x-ray cross sections¹⁶ in a variety of gases up to Xe ($Z = 54$) for 52-MeV Cl. As was done above, extrapolation to 70 MeV was accomplished assuming the velocity dependence of the BEA theory for direct ionization. Linear interpolation between the resulting values, along with a Z^2 extension to $Z = 79$, completed the set of cross sections and yielded the slowly varying curve in Fig. 5(a) for σ_v . Although the measured cross sections¹⁶ indicate an oscillatory behavior on target Z at lower incident energies and hence molecular-orbital promotion as the dominant mechanism, at 52 MeV they have lost most of the oscillation and are starting to reflect the nature of a Coulomb ionization curve. Hence the extrapolation to $Z = 79$, although not certain, is a reasonable way to proceed.

The resulting curve for Y^{eq} in Fig. 7(b), denoted by the solid line, reflects the oscillatory nature of σ_c and in fact matches up well with experiment. This agreement is encouraging in view of the manipulations necessary to obtain the rearrangement cross sections and possible uncertainties therein. If one allows for the uncertainty in the scaling of the BK cross section, for example, using 0.15 in place of 0.07, the dashed curve in Fig. 7(b) is obtained. Another possibility is inflated Cl K fluorescence yields in the Cl K x-ray experiment,¹⁶ which would lead to overestimates for the Cl K -vacancy cross sections. Of course, it is possible that the experimental extrapolation from 140 to 70 MeV to obtain σ_K^x could also lead to some error. In spite of the many difficulties involved in the comparison, it is evident that the vacancy fraction as a function of the Z of the medium exhibits qualitatively the features expected according to the projectile K -shell rearrangement picture.

The cross sections σ_K^x for 64-MeV S and 70-MeV Cl, which were the same for 50- and 100- $\mu\text{g}/\text{cm}^2$ prefoils, were within the experimental repeatability of $\pm 5\%$ equal to those for the K -shell-filled ions, e.g., S^{14+} and Cl^{15+} . Thus the K excitation observed in the solid was eliminated upon emergence from the prefoil, presumably by K x-ray and Auger transitions. Semiempirical estimates¹⁷ for the mean charges are 12.3 and 12.9 for S and Cl, respectively. Although a knowledge of the average fluorescence yields for the highly stripped emerging ions would be needed for a precise determination of the charge change, it is reasonable to conclude that a major portion of the K relaxation would be via Auger emission. For atomic fluorescence yields¹⁸ of 0.082 for S and 0.095 for Cl, the mean charge increases would be ~ 0.9 and ~ 0.6 , respectively, due to the loss of the residual K excitation

built up in the solid. A measurement of either the charge-state distributions or the high-resolution x-ray or Auger spectra for these particular situations is needed in order to make explicit estimates for the inflated fluorescence yields expected, for which increases would correspondingly lower the amount of the charge change.

All of the measurements involving probe layers fail to distinguish between the individual states with K vacancies; i.e., only the total vacancy fraction is observed. The equilibrium processes discussed above should affect in a major way the production of a given state with a K vacancy, in conjunction with similar processes for the outer shells. The measurement of K x rays emitted by metastable states beyond the foil offers an effective way in which to isolate one or a few states, as most of the K transitions will take place within very short distances beyond the foil. Accordingly we show in Fig. 9 for 70-MeV Cl the relative yields of Cl K x rays observed with a Si(Li) detector 1–3 cm beyond C foils of various thicknesses. High-resolution measurements¹⁹ at 50 MeV show that the spectrum in this region consists of two metastable transitions, the three-electron $(1s, 2s, 2p)$ $^4P_{5/2}$ and the two-electron $(1s, 2p)$ 3P_2 decays. Allowing for higher stripping at 70 MeV than 50 MeV, the 3P_2 should be the dominant transition, although we cannot confirm this from our poor resolution spectrum.

Assuming the rearrangement of the outer shells is governed by cross section of the order of 10^{-18} – 10^{-17} cm^2 , the equilibrium occupancy of the Cl L , M , and outer shells should be reached after penetration of ~ 10 $\mu\text{g}/\text{cm}^2$ of C. Beyond that point, the K equilibrium process might be expected to determine the yields of the metastable states. The equilibrium curve in Fig. 9 is the same curve generated for Cl from Eq. (2) reported previously⁷ for the K -vacancy fraction in C. The data have been normalized to the curve at $t = 140$ $\mu\text{g}/\text{cm}^2$,

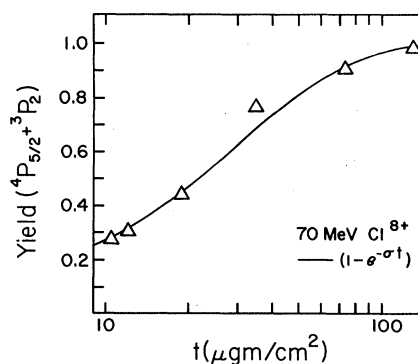


FIG. 9. Cl K metastable production as a function of C foil thickness.

which itself is set to 1.0 at $t = \infty$. The agreement is striking and indicates that K rearrangement does indeed dictate in a straightforward way the formation of individual states with K vacancies, well beyond thicknesses where outer-shell equilibrium should be reached.

2. Fluorine

As can be seen in Fig. 4, only small differences were observed between the σ_x^S and σ_x^E modes, with the 19-MeV points showing the largest effect of $\sim 15\%$. This result implies minimal K relaxation and correspondingly small probability for population of the L and outer shells of the emerging ion as well as the ion in the solid. The current observation is in agreement with an earlier measurement⁵ for 40-MeV O ions moving in Si, which indicated negligible residual O K -shell excitation and hence equivalence of charge-state distributions inside and emerging from the solid. The measurement is to some extent a confirmation of the Bohr criterion² widely used in estimating charge-state distributions; i.e., no shells will be populated whose orbital velocities are less than the projectile velocity. In the present situation the incident velocities are substantially larger than those²⁰ for the F L shell in one-, two-, or multi-electron ions.

The K -vacancy fraction has been determined in the manner used above for the heavier ions,

$$Y(t) = (\sigma_x^S - \sigma_x^{7+}) / \sigma_x^K, \quad (4)$$

where the slight nonlinearity of the increase in the yields from F^{8+} to F^{9+} has been neglected and $\sigma_x^K = \sigma_x^{9+} - \sigma_x^{7+}$. The values of $Y(t)$ measured with the 20- $\mu\text{g}/\text{cm}^2$ foils, determined to be the equilibrium values Y^{eq} by repeating with 50- $\mu\text{g}/\text{cm}^2$ C backings at 19 and 38 MeV, are shown in Fig. 10.

The FK rearrangement cross sections presented in Table II for the relevant energies have been taken from data for capture and loss for F in N_2

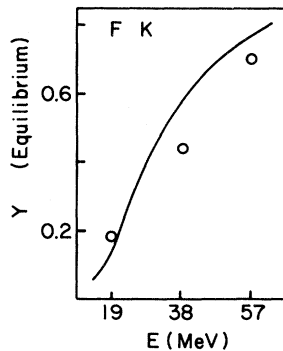


FIG. 10. Energy dependence of Y^{eq} for F in C.

TABLE II. Rearrangement cross sections for F in C.

E (MeV)	σ_v (10^{-18} cm^2)	σ_c (10^{-18} cm^2)
14	0.118	1.86
19	0.304	1.91
38	1.46	1.05
57	2.80	0.81
62	3.10	0.77

under single-collision conditions.²¹ The vacancy cross section σ_v was obtained in the following way. In the manner presented above using a Z^2 dependence for the ionization cross sections, a $(\frac{v}{v_0})^2$ scaling of the electron-loss cross sections by F^{8+} provided a value for the ground-state one-electron ion in C. The behavior of the loss cross section for F^{7+} in N_2 departs markedly from that expected from the F^{8+} points and in fact shows an enhancement which may well reflect effects due to a significantly large $1s2s$ (3S_1) metastable component in the beam,⁹ for which the loss probability should be much larger. In order to get σ_v for a ground-state two-electron ion, we have extended the F^{8+} value by assuming an inverse dependence on the square of the K -shell binding energy.²⁰ Taking the relative fractions of F^{7+} and F^{8+} in measured charge-state distributions²² to be indicative of the distribution in the solid, we obtain an average σ_v which is a weighted sum of the individual cross sections. The values are not greatly different from the F^{8+} values. The σ_c values have been derived by normalizing at several incident energies the BK magnitude¹¹ to the data for F^{9+} in N_2 . The scaling factors obtained were then applied to the BK values for F in C, yielding cross sections for charge exchange into a FK vacancy. The quantity τ has not been measured for F or neighboring ions. However a consideration of the few electron states expected in the solid at the current energies and the experimental results⁶ for S, where the average τ was a factor of 10 below the single-vacancy rate would indicate that an upper limit of $\sim 5 \times 10^{-13}$ sec is reasonable. As the corresponding σ_τ is substantially smaller than the cross sections for σ_v and σ_c , we have neglected here that contribution to the rearrangement. The solid curve for $Y^{\text{eq}} = \sigma_v / (\sigma_v + \sigma_c)$ in Fig. 10 describes well the behavior of the experimental points.

It is interesting to note in this particular situation that the emerging charge-state distribution itself is determined primarily by the K equilibrium process, with limited participation by outer electrons. Hence Dmitriev²³ was able to predict with surprising accuracy the mean charge of F and lighter ions emerging from C foils simply by in-

voking the Bohr criterion and extrapolating measured electron-loss probabilities taken from equilibrium values of the H^+ and H^0 fractions in gases. In view of the great disparity between the HK and the FK binding energies and the many deviations of the measured ionization²⁴ and electron-capture^{12,21} cross sections from the simplest expectations where heavy ions are concerned, the success of that approach is rather amazing.

As mentioned before, the charge-state dependence in Fig. 4 is very similar to that reported by Brandt *et al.*⁴ for O ions. The latter group observed that the dependence was reduced as the Al thickness was increased; i.e., the various yields converged to a mean yield associated with an equilibrium distribution in the solid. We show in Fig. 11 the F-induced Al K x-ray cross sections for the $1\text{-}\mu\text{g}/\text{cm}^2$ target, along with the relative cross sections recorded for a $10\text{-}\mu\text{g}/\text{cm}^2$ Al target. As with O, the individual charge states produced yields from the thicker target which cluster around some mean value, hence represent beams which have thoroughly equilibrated in the Al. Brandt *et al.* suggested that the reduction of the yield with O^{8+} was due to the establishment of a polarization cloud of electrons from the conduction band around the ion which screened the medium from the nuclear charge and so reduced the Al K x-ray cross sections. The response time, determined by the plasma frequency of Al, should be on the order of 10^{-16} sec. The preceding information in this

section indicates that an alternative explanation is that the fully stripped F or O simply equilibrates to a charge-state distribution with a K vacancy fraction <1 , depressing the Al K yield.

In order to distinguish between the two possibilities—screening vs equilibrium population of the K shell—we repeated the measurement with a C prefoil in, e.g., the σ_x^E mode. Since the measured equilibrium charge-state distributions are nearly identical²² for O(F) in C and Al, such a procedure removes effects due to the K equilibrium process. The emerging beam, itself of a high mean charge²² around 7^+ at 19 MeV or 8^+ at 57 MeV, should initiate the screening process upon entering the Al, causing a reduction in the yield from the thicker Al target. The results are shown in Fig. 12 along with the values for F^{9+} from Fig. 11. It is clear that the reaching of charge state equilibrium, specifically K equilibrium, accounts for the decreased yields. The thin- and thick-target cross sections are about equal once that process is complete, i.e., screening effects are not significant. This is not to say that a polarization cloud does not exist. The point is that over the present projectile velocities there is no significant effect on the Al K x-ray cross section, i.e., close collisions, due to an enhanced electron density of that type. This result is in agreement with recent experimental findings²⁵ that indicate stopping powers of channeled 28-MeV oxygen ions in Ag do not show significant screening effects, i.e., even where distant collisions are involved.

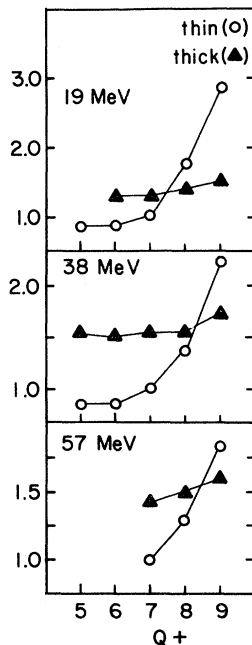


FIG. 11. Thin and thick Al target yields for various F charge states.

IV. DISCUSSION

The accuracy of the simple approach represented by Eq. (2) in describing the above experimental results qualitatively and in most cases quantitatively is an encouraging step in attempts to determine the states of ions moving inside solids.

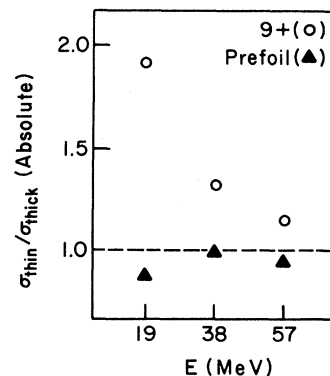


FIG. 12. Ratio of thin to thick yields with and without C prefoil stripping.

The successful application of the most straightforward rearrangement cross sections, often measured with thin gas targets under single-collision conditions, to the multiple collisions situation encountered in the dense environment of the solid provides a basis for unraveling some of the complexity of that situation. A complementary step is the quantitative determination of the production of individual states, such as the measurement of metastables provides. Such an investigation has been reported recently.²⁶

The technique of using very thin probe layers can be extended to measuring vacancy fractions for any given shell, provided that the x-ray cross section is sensitive primarily to the occupancy of that shell and the rearrangement within the probe layer is either negligible or well understood over the given thickness. Further, one can make theoretical estimates for vacancy fractions to the extent that accurate rearrangement cross sections are known. The problem of determining the total electron configurations even in an average way, i.e., the numbers of electrons in each major shell, must be solved before the extent to which the BL and BG models accurately describe the total situation for the heavier ions investigated here can be determined.

There are several implications of the measurement presented in this paper which we should like to emphasize by way of briefly mentioning them. Perhaps the most obvious is the thickness dependence of projectile and target vacancy cross sections and the x-ray or Auger emission resulting. Such effects have been studied several times before⁴⁻⁶ and again more recently.²⁷ For example,

if a target vacancy cross section is highly dependent on the number of vacancies in a particular shell of the projectile, the cross sections measured using solid targets can show enhancements and equilibrium effects even when emerging charge distributions at the same energy have no significant vacancies in that shell. The possibility of residual excitation must be addressed when data are interpreted, particularly where heavy ions are used. The same considerations apply to other phenomena involving inner-shell vacancies, such as the anomalous transient field effect²⁸ in the hyperfine interaction of heavy ions recoiling at high velocities ($\approx 0.03c$) in polarized iron. The latter effect has been characterized as being due to polarized electrons captured into the inner *s* shells and would thereby depend directly on the vacancy fractions of those shells.

Certain practical experimental consequences arise from the equilibrium processes discussed here. In beam-foil studies of metastable states with inner-shell vacancies, the yields of x rays or Auger electrons may be thickness dependent for relatively thick stripping foils, e.g., the $\sim 100 \mu\text{g}/\text{cm}^2$ C foils used here to observe Cl *K* x rays. The determination of the maximum production of a particular state, an important aspect where data taking is restricted in time as at many accelerator facilities, requires a careful check of equilibrium thicknesses. Similarly the mean charges for the heavier ions such as S and Cl here at several MeV/amu energies may increase noticeably with thicker strippers, with a corresponding increase in the higher charge states of the emerging charge-state distributions.

*Supported in part by the National Science Foundation.

¹H. D. Betz, *Rev. Mod. Phys.* **44**, 465 (1972).

²N. Bohr and J. Lindhard, *K. Dan. Vidensk. Selsk. Mat.-Fys. Medd.* **28**, No. 7 (1954).

³H. D. Betz and L. Grodzins, *Phys. Rev. Lett.* **25**, 211 (1970).

⁴W. Brandt, R. Laubert, M. Maurino, and A. Schwarzschild, *Phys. Rev. Lett.* **30**, 358 (1973).

⁵S. Datz, B. R. Appleton, J. R. Mowat, R. Laubert, R. S. Peterson, R. S. Thoe, and I. A. Sellin, *Phys. Rev. Lett.* **33**, 733 (1974); and H. O. Lutz, J. Stein, S. Datz, and C. D. Moak, *Phys. Rev. Lett.* **28**, 8 (1972).

⁶H. D. Betz, F. Bell, H. Panke, G. Kalkoffen, M. Welz, and D. Evers, *Phys. Rev. Lett.* **33**, 807 (1974).

⁷F. Hopkins, *Phys. Rev. Lett.* **35**, 270 (1975).

⁸R. J. Fortner and J. D. Garcia, *Phys. Rev. A* **12**, 856 (1975).

⁹R. J. Fortner and D. L. Matthews, in *Proceedings of the Fourth International Conference on Beam-Foil Spectroscopy and Heavy-Ion Atomic Physics, Gatlinburg, Tenn., 1975* (Plenum, New York, 1976).

¹⁰F. Hopkins, N. Cue, and V. Dutkiewicz, *Phys. Rev. A* **12**, 1710 (1975).

¹¹V. S. Nikolaev, *Zh. Eksp. Teor. Fiz.* **51**, 1263 (1966) [*Sov. Phys.-JETP* **24**, 847 (1967)].

¹²F. Hopkins, R. Brenn, A. R. Whitemore, N. Cue, V. Dutkiewicz, and R. P. Chaturvedi, *Phys. Rev. A* **13**, 74 (1976).

¹³F. Hopkins, R. Brenn, A. Whitemore, N. Cue, and V. Dutkiewicz, *Phys. Rev. A* **11**, 1482 (1975).

¹⁴J. H. McGuire and P. Richard, *Phys. Rev. A* **8**, 1374 (1973).

¹⁵E. J. McGuire, *Phys. Rev.* **185**, 1 (1969).

¹⁶L. Winters, M. D. Brown, L. D. Ellsworth, T. Chiao, E. W. Pettus, and J. R. Macdonald, *Phys. Rev. A* **11**, 174 (1975).

¹⁷I. S. Dmitriev and V. S. Nikolaev, *Zh. Eksp. Teor. Fiz.* **47**, 615 (1964) [*Sov. Phys.-JETP* **20**, 409 (1965)].

¹⁸W. Bambynek, B. Crasemann, R. W. Fink, H. U. Freund, H. Mark, C. D. Swift, R. E. Prince, and P. V. Rao, *Rev. Mod. Phys.* **44**, 716 (1972).

¹⁹C. L. Cocke, B. Curnutte, J. R. Macdonald, and

- R. Randall, *Phys. Rev. A* 9, 57 (1974).
- ²⁰R. L. Kauffman, C. W. Woods, F. F. Hopkins, D. O. Elliott, K. A. Jamison, and P. Richard, *J. Phys. B* 6, 2197 (1973).
- ²¹J. R. Macdonald, S. M. Ferguson, T. Chiao, L. D. Ellsworth, and S. A. Savoy, *Phys. Rev. A* 5, 1188 (1972).
- ²²A. B. Wittkower and H. D. Betz, *At. Data* 5, 113 (1973).
- ²³I. S. Dmitriev, *Zh. Eksp. Teor. Fiz.* 32, 570 (1957) [*Sov. Phys.-JETP* 5, 473 (1957)].
- ²⁴J. D. Garcia, R. J. Fortner, and T. M. Kavanagh, *Rev. Mod. Phys.* 45, 111 (1973); Q. C. Kessel and B. Fastrup, *Case Stud. At. Phys.* 3, 137 (1973).
- ²⁵S. Datz, Proceedings of the Third Conference on Application of Small Accelerators, North Texas State University, 1974, edited by J. L. Duggan and I. L. Morgan, p. 410 (unpublished).
- ²⁶S. L. Varghese, C. L. Cocke, B. Curnutte, and G. G. Seaman, *Bull. Am. Phys. Soc.* 21, 698 (1976).
- ²⁷T. J. Gray, P. Richard, K. A. Jamison, and J. M. Hall, *Bull. Am. Phys. Soc.* 21, 651 (1976); K. O. Groeneveld, B. Kolb, J. Schader, and K. D. Sevier, *Z. Phys. A* 277, 13 (1976).
- ²⁸L. Eberhardt, G. Van Middelkoop, R. E. Horstman, and H. A. Doubt, *Phys. Lett.* 56B, 329 (1975); M. Forterre, J. Gerber, J. P. Vivien, M. B. Goldberg, K.-H. Speidel, and P. N. Tandon, *Phys. Rev. C* 11, 1976 (1975).